Single top plus Higgs at LHC with CP violating top Yukawa

HIGGS 2024

Ya-Juan Zheng
(Iwate University)

November 6, 2024

Based on [1] Vernon Barger, Kaoru Hagiwara and YJZ, Phys.Rev.D 99 (2019) 3,031701.
[2] Vernon Barger, Kaoru Hagiwara and YJZ, JHEP09(2020) 176.
[3] Vernon Barger, Kaoru Hagiwara and YJZ, in preparation

Outline

- CPV top-Yukawa coupling from an effective Lagrangian
- Helicity amplitudes: ub > dth for $pp \to thj$
- Single top/anti-top + Higgs event distributions
- Azymuthal asymmetry $A_\phi(\bar{A}_\phi)$ in $pp \to thj(\bar{t}hj)$ events
- Top (anti-top) polarisation $P_2(\bar{P}_2)$ in $pp \to thj(\bar{t}hj)$ events
- Summary

LHC searches and constraints

$$\mathcal{L}_{ttH} = -gH\bar{t}(\cos\xi + i\gamma_5 \sin\xi)t$$

g is real and positive, -π < ξ< π

When $g=g_{SM}=m_t/v$, ξ=0 ⟶ SM

- X. Zhang, S. K. Lee, K. Whisnant, and B. L. Young, "Phenomenology of a nonstandard top quark Yukawa coupling," Phys. Rev. D 50 (1994) 7042–7047, arXiv:hep-ph/9407259.
- H. Bahl, E. Fuchs, S. Heinemeyer, J. Katzy, M. Menen, K. Peters, M. Saimpert, and G. Weiglein, "Constraining the CP structure of Higgs-fermion couplings with a global LHC fit, the electron EDM and baryogenesis," Eur. Phys. J. C 82 (2022) no. 7, 604, arXiv:2202.11753 [hep-ph].
- …

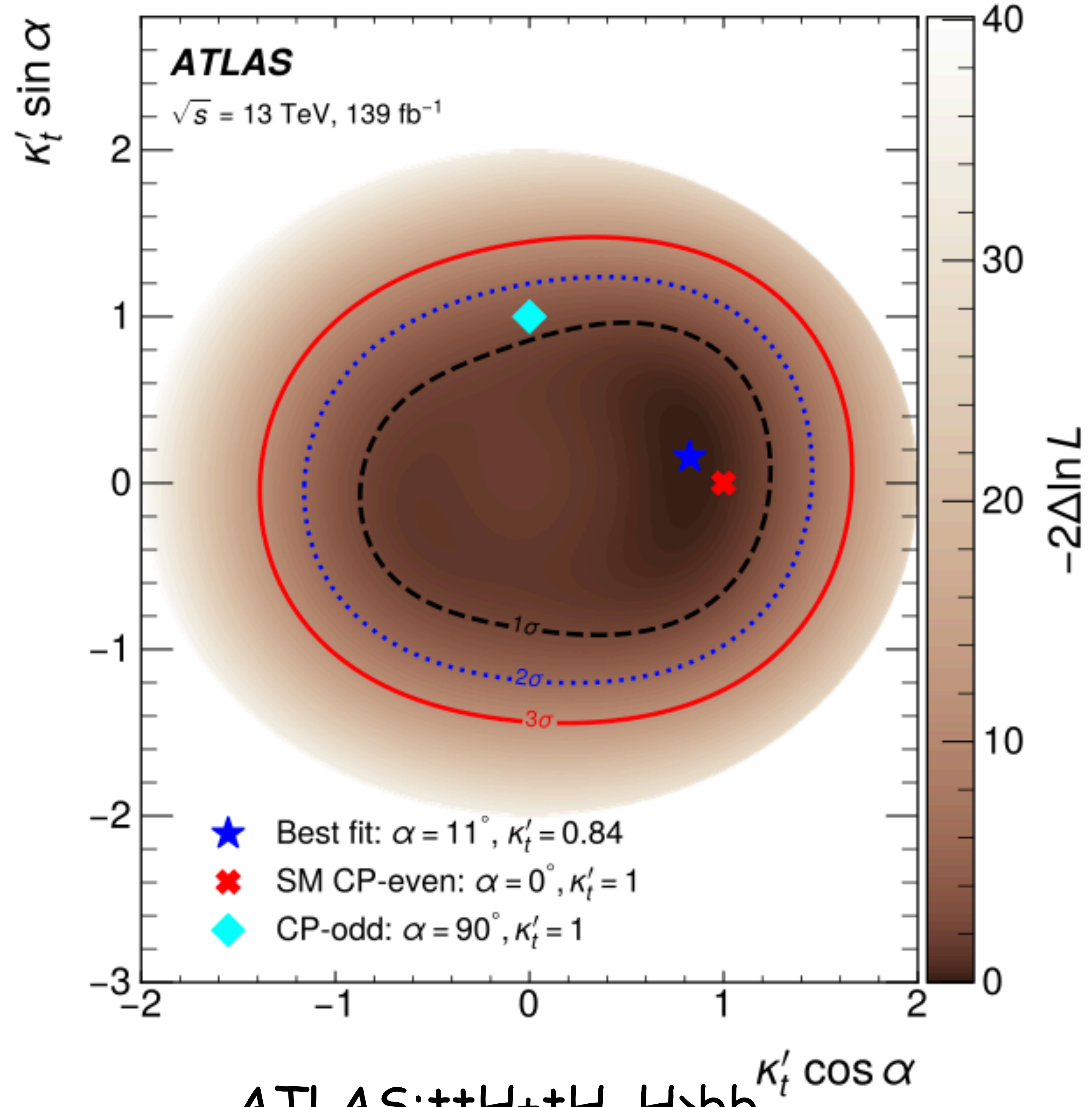

ATLAS:ttH+tH, H>bb
arXiv:2303.05974

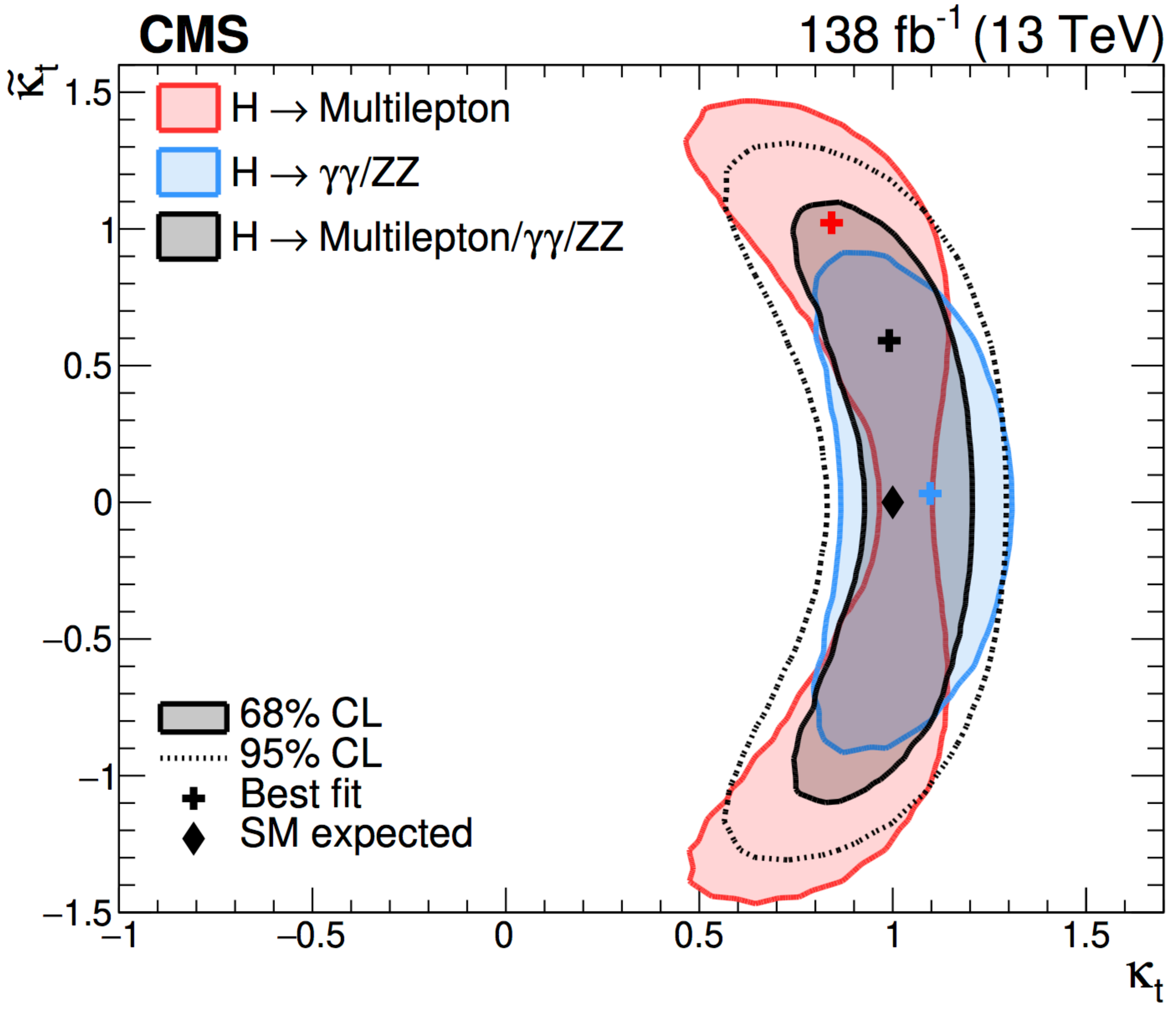

CMS:ttH+tH, H>ls/rr/ZZ
JHEP07(2023)092

LHC direct searches:
ATLAS best fit:11+52-73 degree

CP-violating top Yukawa coupling

kappa framework

$$\mathcal{L} = -g_{htt} h \bar{t} \left(\cos\xi_{htt} + i \sin\xi_{htt}\gamma_5\right) t$$
$$= -g_{htt} h (t_R^\dagger, t_L^\dagger) \begin{pmatrix} e^{-i\xi_{htt}} & 0 \\ 0 & e^{i\xi_{htt}} \end{pmatrix} \begin{pmatrix} t_L \\ t_R \end{pmatrix}$$
$$= -g_{htt} h (e^{-i\xi_{htt}} t_R^\dagger t_L + e^{i\xi_{htt}} t_L^\dagger t_R)$$

$$g_{htt} = \frac{m_t}{v}\kappa_{htt}, \qquad \kappa_{htt} > 0, \qquad -\pi < \xi_{htt} \leq \pi$$

Gauge invariant Lagrangian with dimension six operator in SMEFT:

$$\mathcal{L} = -y_{\rm SM} Q^\dagger \phi t_R + \frac{\lambda}{\Lambda^2} Q^\dagger \phi t_R \left(\phi^\dagger\phi - \frac{v^2}{2}\right) + \text{h.c.}$$
$$Q = (t_L, b_L)^T$$
$$\phi = ((v + H + i\pi^0)/\sqrt{2}, i\pi^-)^T$$
$$g_{\rm SM} = \frac{y_{\rm SM}}{\sqrt{2}} = \frac{m_t}{v} \qquad \frac{g_{\rm SM} - g e^{i\xi}}{v^2} = \frac{\lambda}{\Lambda^2}$$

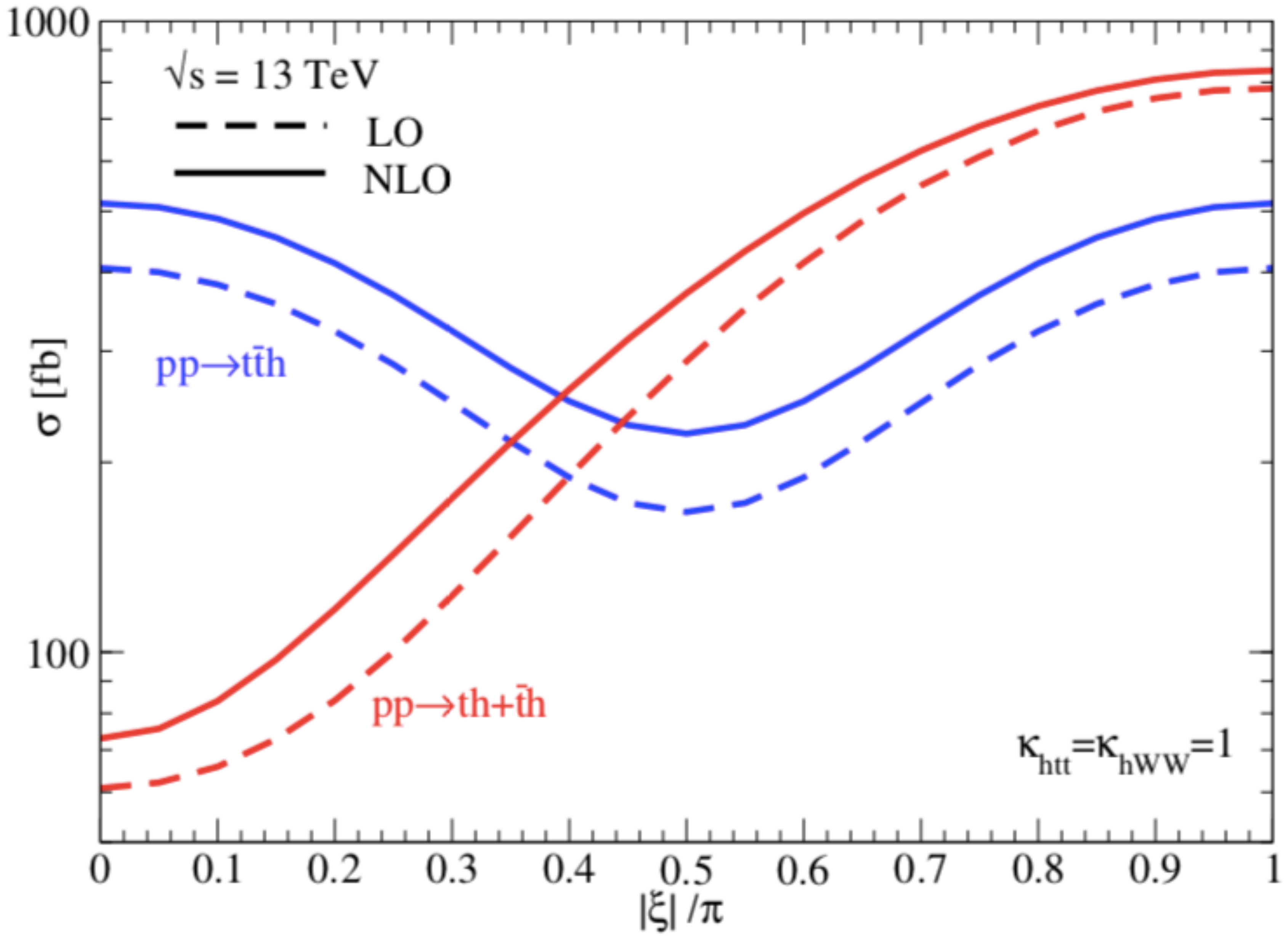

$$pp \to th + \bar{t}h + \text{anything}$$

$$\sigma_{tot}(|\xi_{htt}| = \pi) \sim 13\ \sigma_{tot}^{SM}(\xi_{htt} = 0)$$

change the sign of Yukawa coupling

In the SM, strong destructive interference between the htt and hWW amplitudes.

Preserving unitarity

W.Stirling, D.Summers, Phys.Lett.B283(1992)411-415
G.Bordes,B.van Eijk, Phys.Lett.B299(1993)315-320

ub > dth amplitudes in unitary gauge

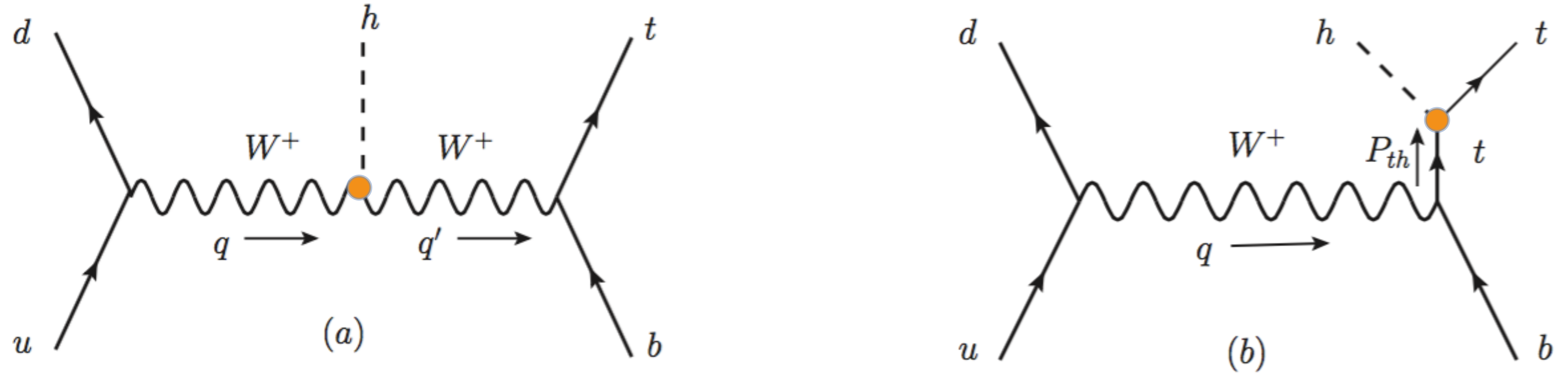

$$M_\sigma \sim u_L(p_d)^\dagger \sigma_-^\mu u_L(p_u) \frac{-g_{\mu\nu} + q_\mu q_\nu / m_W^2}{q^2 - m_W^2}$$

common to both diagrams

$$\left(u_R^\dagger(p_t,\sigma), u_L^\dagger(p_t,\sigma)\right) \left\{ g_{hWW} \frac{-g_\rho^\nu + q'^\nu q'_\rho / m_W^2}{q'^2 - m_W^2} + \frac{g_{htt}\delta_\rho^\nu}{P_{th}^2 - m_t^2} \begin{pmatrix} e^{-i\xi} & 0 \\ 0 & e^{i\xi} \end{pmatrix} \begin{pmatrix} m & P_{th}\cdot\sigma_+ \\ P_{th}\cdot\sigma_- & m \end{pmatrix} \right\} \begin{pmatrix} 0 & \sigma_+^\rho \\ \sigma_-^\rho & 0 \end{pmatrix} \begin{pmatrix} u_L(p_b) \\ 0 \end{pmatrix}$$

$\bar{u}(p_t,\sigma)$

$\cos\xi + i\sin\xi\gamma_5$

$P_{th}\cdot\gamma + m$

γ^ρ

$\frac{1-\gamma_5}{2} u(p_b)$

$$g_{hWW} = \frac{2m_W^2}{v}\kappa_{hWW} \quad (\kappa_{hWW} = 1)$$

Amplitudes (full process u b > d t h)

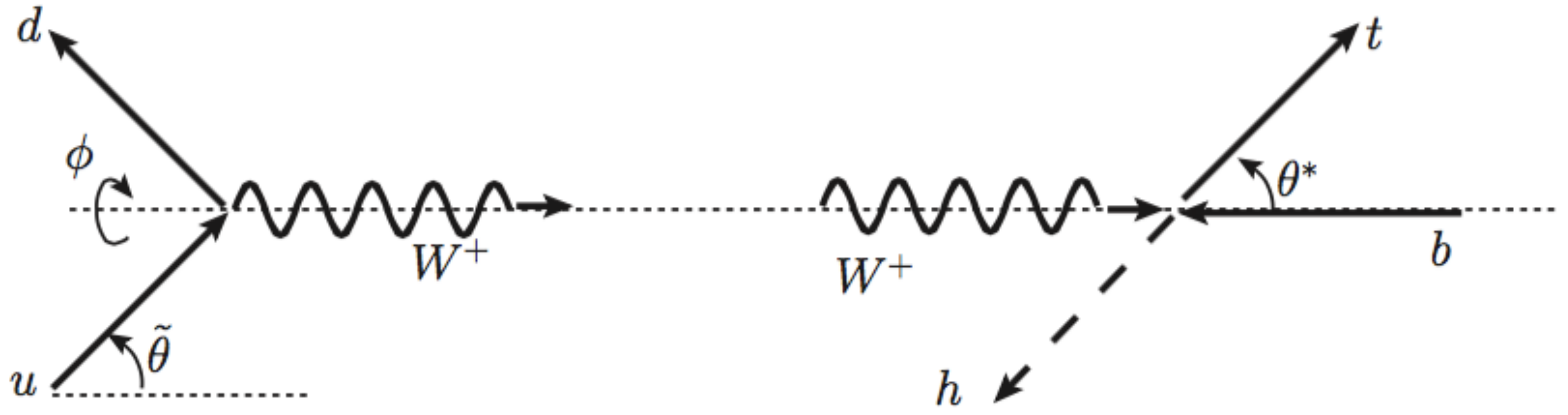

we choose the weak boson momentum direction in the Wb>th rest frame as the z axis

$$M_\sigma = \sum_{\lambda=\pm1,0} j(u \to dW^+_\lambda)\ \hat{M}(W^+_\lambda b \to t_\sigma h)$$

$$M_+ = \frac{1-\tilde{c}}{2} e^{i\phi} \sin\frac{\theta^*}{2} A \frac{1+\cos\theta^*}{2}$$ ← λ=+1, Jz=3/2

$$+ \frac{1+\tilde{c}}{2} e^{-i\phi} \sin\frac{\theta^*}{2} \left[A\left(\frac{1+\cos\theta^*}{2} + \epsilon_1\right) - B\left(e^{-i\xi} + \delta\delta' e^{i\xi}\right)\right]$$ ← λ=-1, Jz=-1/2

$$+ \frac{\tilde{s}}{2} \cos\frac{\theta^*}{2} \frac{W}{Q} \left[A\left(\frac{q^* E_h^* + q^{0*} p^* \cos\theta^*}{W p^*} + \epsilon_1\right) - B\left(e^{-i\xi} + \delta\delta' e^{i\xi}\right)\right]$$ ← λ=0, Jz=1/2

$$M_- = -\frac{1-\tilde{c}}{2} e^{i\phi} \cos\frac{\theta^*}{2} A\delta \frac{1-\cos\theta^*}{2}$$ ← λ=+1, Jz=3/2

$$- \frac{1+\tilde{c}}{2} e^{-i\phi} \cos\frac{\theta^*}{2} \left[A\left(\delta\frac{1-\cos\theta^*}{2} - \epsilon_2\right) + B\left(\delta e^{-i\xi} + \delta' e^{i\xi}\right)\right]$$ ← λ=-1, Jz=-1/2

$$- \frac{\tilde{s}}{2} \sin\frac{\theta^*}{2} \frac{W}{Q} \left[A\left(\delta\frac{q^* E_h^* + q^{0*} p^* \cos\theta^*}{W p^*} + \epsilon_2\right) + B\left(\delta e^{-i\xi} + \delta' e^{i\xi}\right)\right]$$ ← λ=0, Jz=1/2

$$A = 2g^2 D_W(q) \tilde{\omega} \sqrt{2q^*(E^*+p^*)} \frac{mp^*}{m_W^2} g_{hWW} D_W(q'),$$ >0

$$B = -2g^2 D_W(q) \tilde{\omega} \sqrt{2q^*(E^*+p^*)} W g_{htt} D_t(P_{th}),$$ >0

$$\delta = m_t/(E^* + p^*)$$

$$\delta' = m_t/W$$

→ δ ~ δ' at high energy high W ($W=m_{th}$)

Q and W distribution

$Q = \sqrt{-q^2}$ invariant momentum transfer of the virtual W^+

$W = \sqrt{P_{th}^2} = m(th)$ the invariant mass of the th system

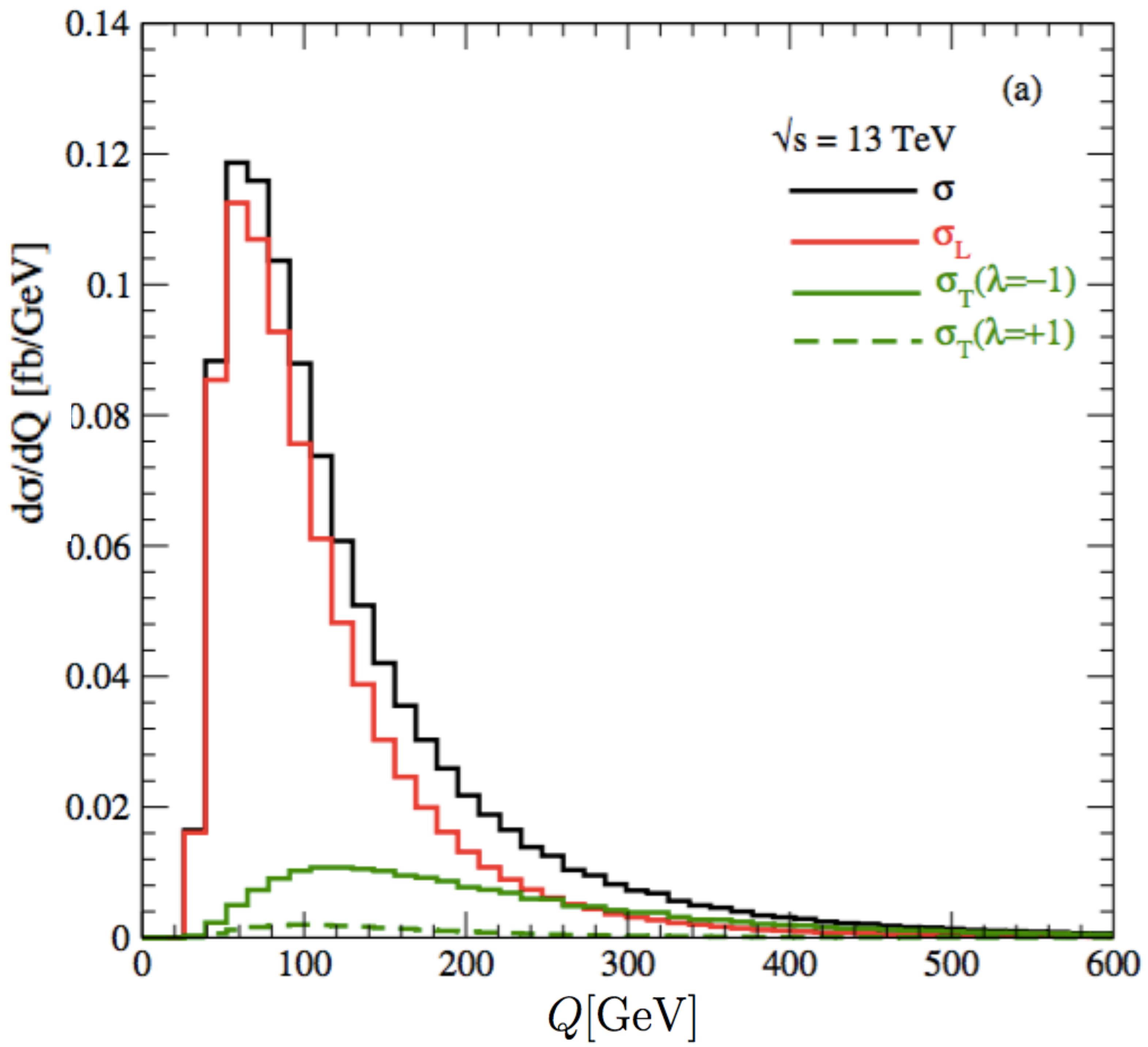

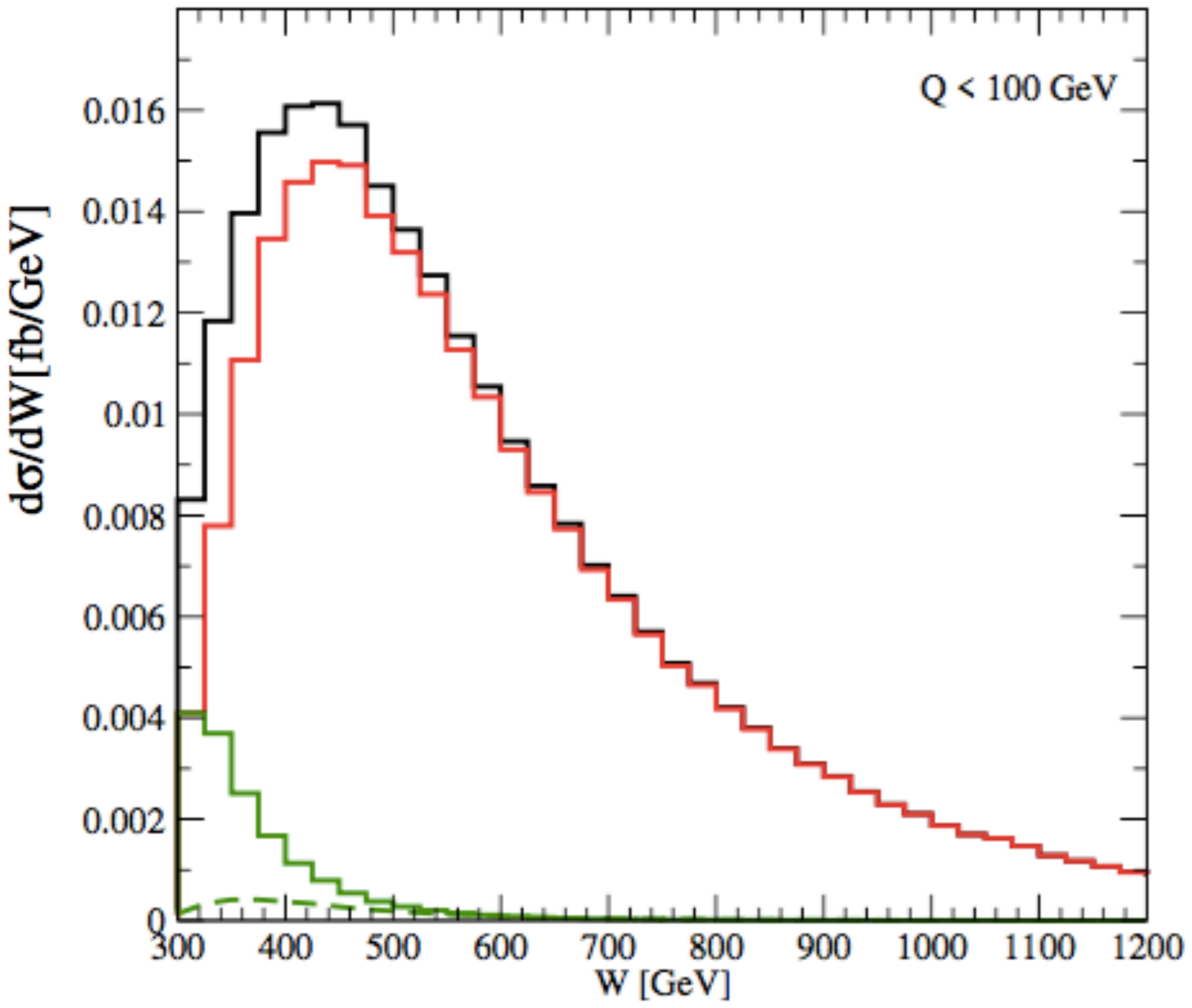

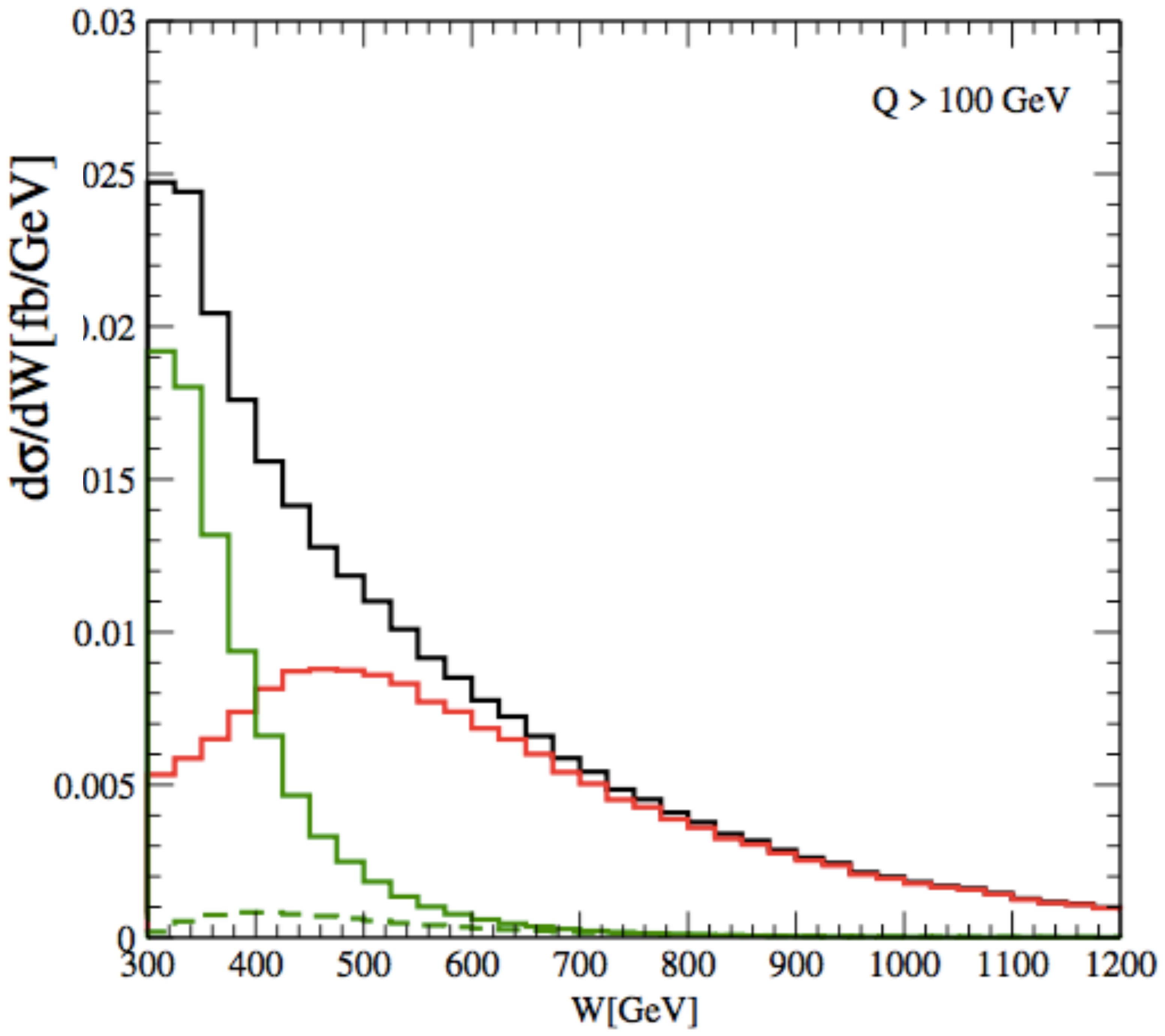

W_L is dominant in low Q (Q<100 GeV) and large W (W>400 GeV) —> top polarization asymmetry

W_T is significant in large Q (Q>100 GeV) and small W (W<400 GeV) —> azimuthal asymmetry

Azimuthal angle distribution

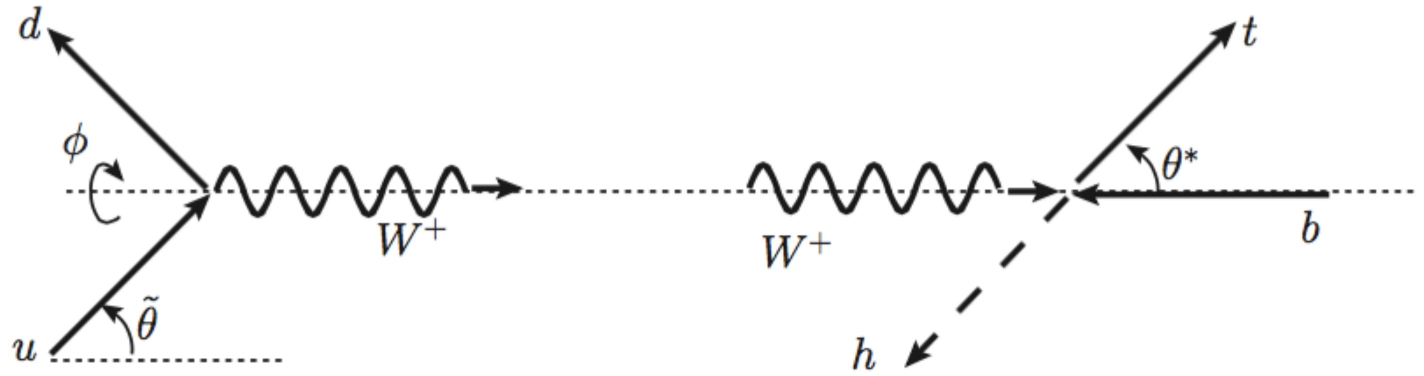

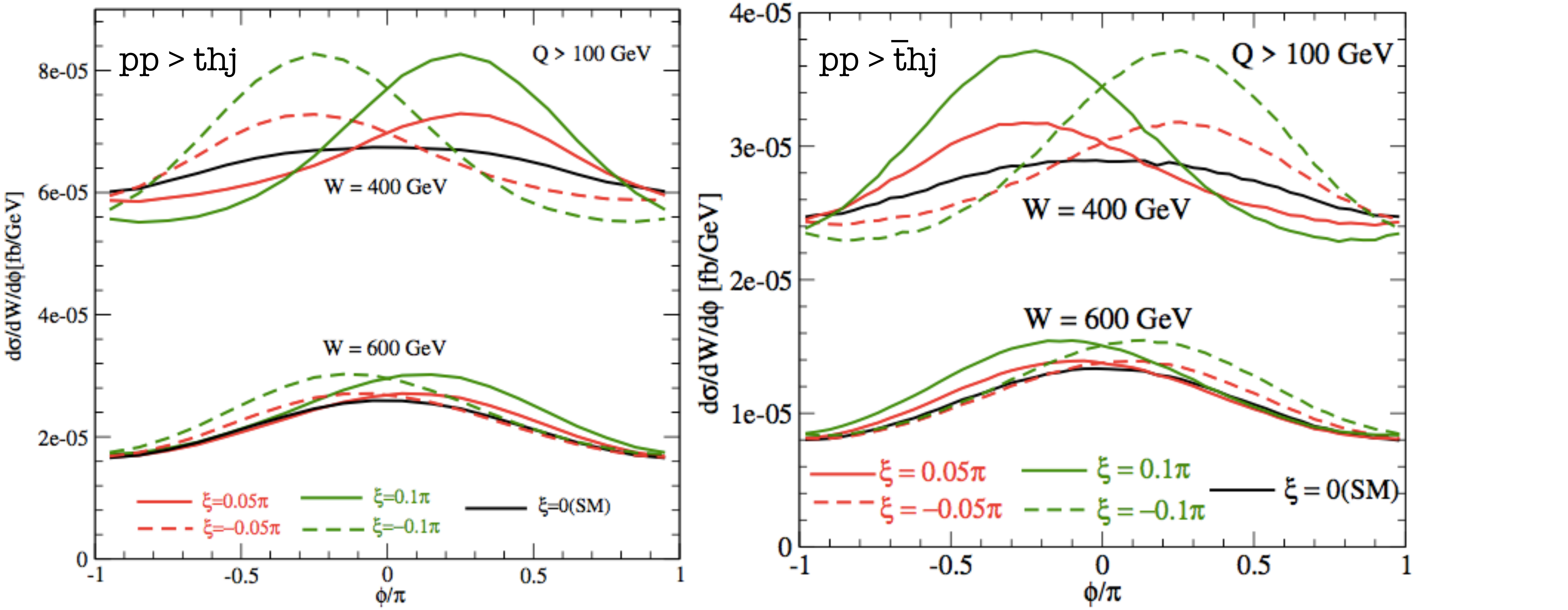

FIG. 8: Left panel: t. Right panel: $\bar{t}$. $d\sigma/d\mathtt{W}/d\phi$ v.s. ϕ at $\mathtt{W} = 400$ and 600 GeV for $Q > 100$ GeV. Black, red and green curves are for the SM ($\xi = 0$), $\xi = \pm 0.1\pi$, and $\pm 0.2\pi$. The solid curve are for $\xi \geq 0$, while the dashed curves are for $\xi < 0$.

asymmetry

$$A_\phi(\mathtt{W}) = \frac{\int_{-\pi}^{\pi} d\phi \, \mathrm{sgn}(\phi) d\sigma/d\mathtt{W}/d\phi}{d\sigma/d\mathtt{W}}$$

$> 0 \ (th)$ and $< 0 \ (\bar{t}h)$ for $\xi > 0$

$< 0 \ (th)$ and $> 0 \ (\bar{t}h)$ for $\xi < 0$

Asymmetry is large at small W & large Q (W_T is comparable to W_L)
small at large W & small Q (W_L dominates over W_T)

Azimuthal asymmetry A_φ

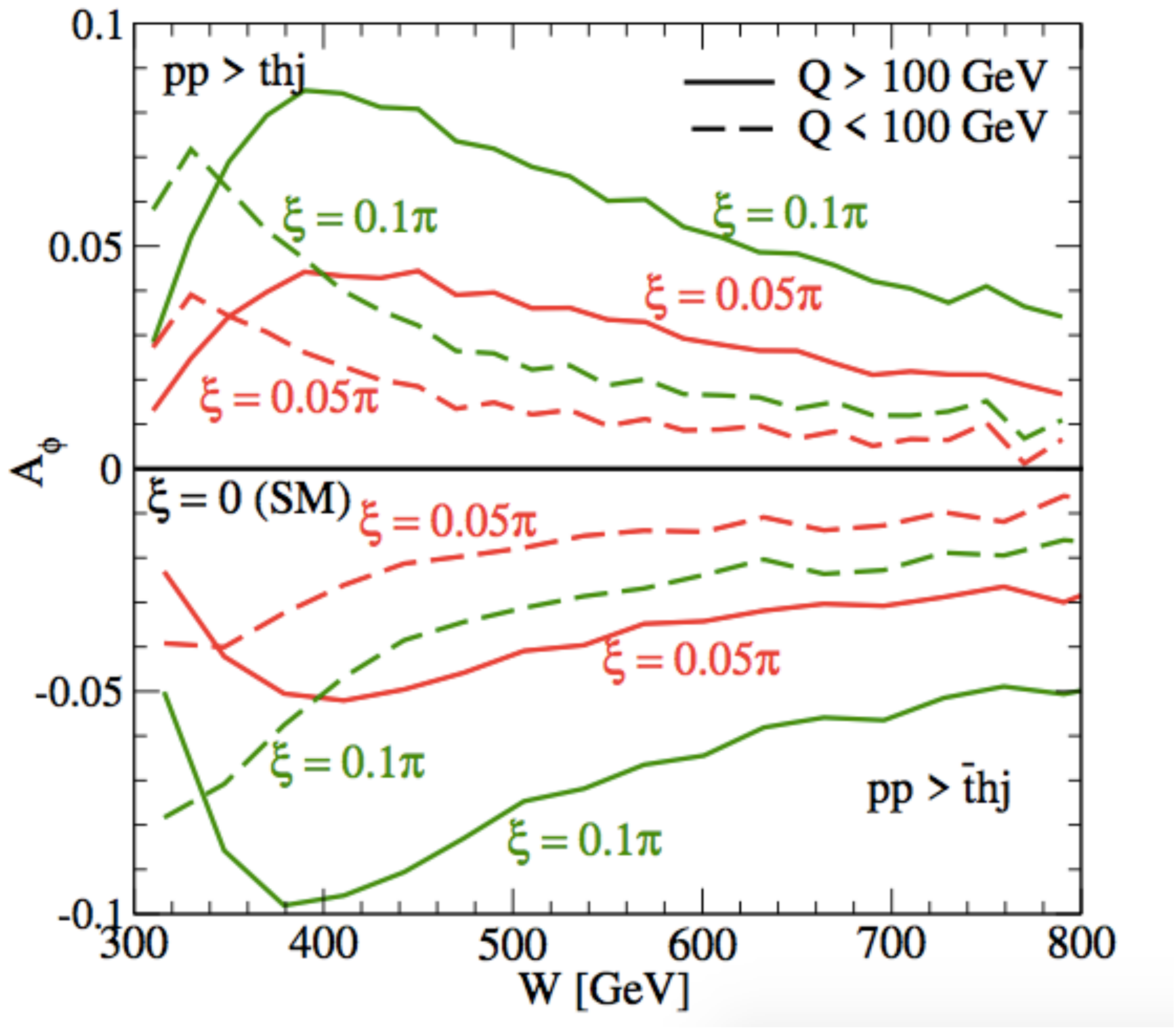

FIG. 11: Asymmetry $A_\phi(W)$ for $pp \to thj$ and $pp \to \bar{t}hj$ as functions of W, the invariant mass of th or $\bar{t}h$ system. Large Q ($Q > 100$ GeV) events are shown by solid lines, while small Q ($Q < 100$)GeV, events are shown by dashed curves. Results are shown for $\xi = 0$ (SM), $\xi = 0.05\pi$ (red) and 0.1π (green). $A_\phi > 0$ for th and $A_\phi < 0$ for $\bar{t}h$, when $\xi > 0$.

$|\mathcal{M}_+(ub > dth)|^2$ v.s. $|\overline{\mathcal{M}}_-(d\bar{b} > u\bar{t}h)|^2$

$$\mathcal{M}_+ = \frac{1-\tilde{c}}{2} e^{i\phi} \sin\frac{\theta^*}{2} \left[\frac{1+\cos\theta^*}{4} \bar{\beta} A \right]$$

$J_Z=3/2$, $\lambda=+1$

$$+ \frac{1+\tilde{c}}{2} e^{-i\phi} \sin\frac{\theta^*}{2} \left[\left(\frac{1+\cos\theta^*}{4}\bar{\beta} + \epsilon\delta\delta' \right) A - \left(e^{-i\xi} + \delta\delta' e^{i\xi} \right) B \right]$$

$J_Z=-1/2$, $\lambda=-1$

$$+ \frac{\tilde{s}}{2} \frac{W}{Q} \cos\frac{\theta^*}{2} \left[\left(\frac{q^* E_h^* + q^{0*} p^* \cos\theta^*}{W^2} + \epsilon\delta\delta' \right) A - \left(e^{-i\xi} + \delta\delta' e^{i\xi} \right) B \right]$$

$J_Z=1/2$, $\lambda=0$

$$\overline{\mathcal{M}}_- = \frac{1-\tilde{c}}{2} e^{i\phi} \sin\frac{\theta^*}{2} \left[\left(\frac{1+\cos\theta^*}{4}\bar{\beta} + \epsilon\delta\delta' \right) A - \left(e^{i\xi} + \delta\delta' e^{-i\xi} \right) B \right]$$

$J_Z=1/2$, $\lambda=+1$

$$+ \frac{1+\tilde{c}}{2} e^{-i\phi} \sin\frac{\theta^*}{2} \frac{1+\cos\theta^*}{4} \bar{\beta} A$$

$J_Z=-3/2$, $\lambda=-1$

$$+ \frac{\tilde{s}}{2} \frac{W}{Q} \cos\frac{\theta^*}{2} \left[\left(\frac{q^* E_h^* + q^{0*} p^* \cos\theta^*}{W^2} + \epsilon\delta\delta' \right) A - \left(e^{i\xi} + \delta\delta' e^{-i\xi} \right) B \right]$$

$J_Z=1/2$, $\lambda=0$

Top Polarization (mixed state)

For general mixed state, $|t\rangle = \frac{\mathcal{M}_+ \left|J_z = +\frac{1}{2}\right\rangle + \mathcal{M}_- \left|J_z = -\frac{1}{2}\right\rangle}{\sqrt{|\mathcal{M}_+|^2 + |\mathcal{M}_-|^2}}$ we introduce differential cross section matrix

$$d\sigma_{\lambda\lambda'} = \int dx_1 \int dx_2 D_{u/p}(x_1) D_{b/p}(x_2) \frac{1}{2\hat{s}} \overline{\sum} M_\lambda M^*_{\lambda'} d\Phi_{dth}$$

where the phase space integration can be restricted. For an arbitrary kinematical distributions, $d\sigma = d\sigma_{++} + d\sigma_{--}$ the polarisation density matrix is defined as

$$\rho_{\lambda\lambda'} = \frac{d\sigma_{\lambda\lambda'}}{d\sigma_{++} + d\sigma_{--}} = \frac{1}{2}\left[\delta_{\lambda\lambda'} + \sum_{k=1}^{3} P_k \sigma^k_{\lambda\lambda'}\right]$$

The 3-vector **P** =(P_1,P_2,P_3) gives the general polarisation of the top quark. The magnitude P = |**P**| gives the degree of polarisation (P=1 for 100% polarization, P=0 for no polarisation). The orientation gives the direction of the top quark spin in the top rest frame.

$$P_2 = -2\mathrm{Im}(M_+ M_-^*)/(|M_+|^2 + |M_-|^2)$$

We find **P** lies in the W+b>th scattering plane in the SM (xi=0). Polarisation orthogonal to the production plane P_2 appears for nonzero xi. The sign of P_2 determines the sign of xi.

Top Polarization and anti-top polarisation $P = (P_1, P_2, P_3)$

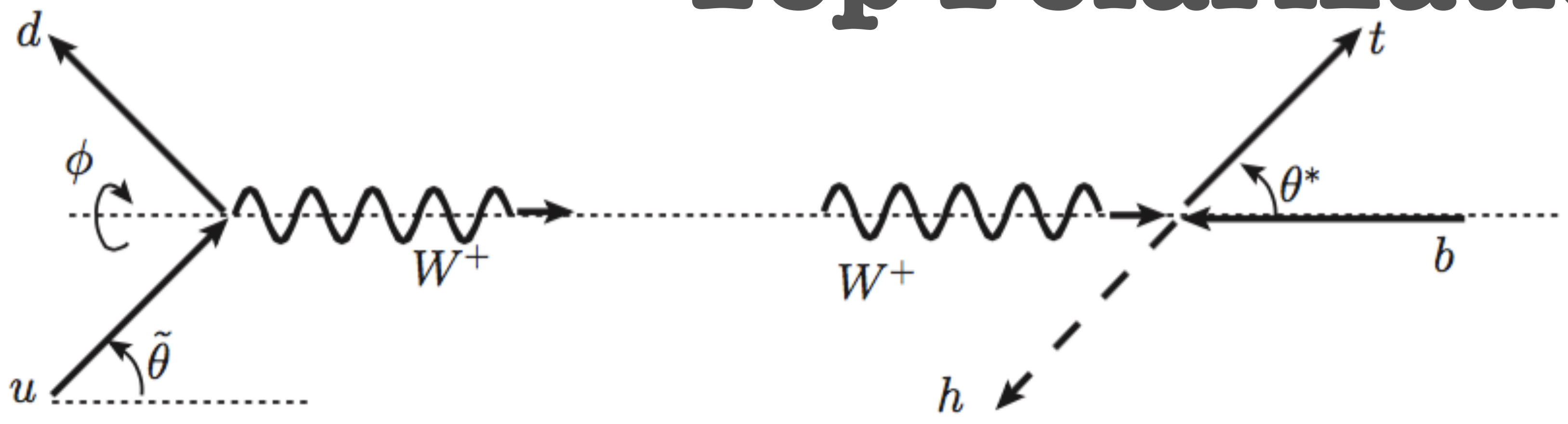

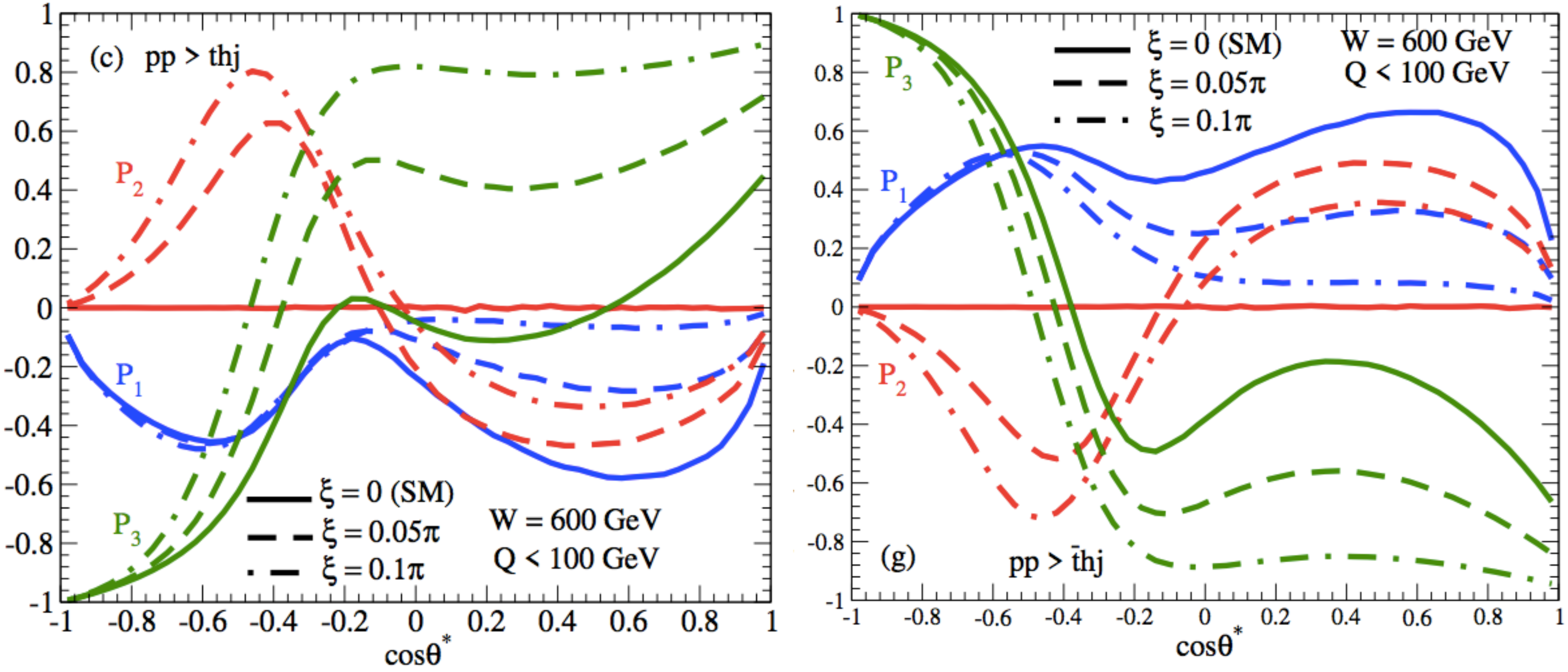

xi=0, P2=0
We find large $|P_2|$ when cosθ*<0, positive for t and negative for tbar. We therefore examine P_2 for events with cosθ*<0 in the next slides.

Polarization P_2 of top and anti-top

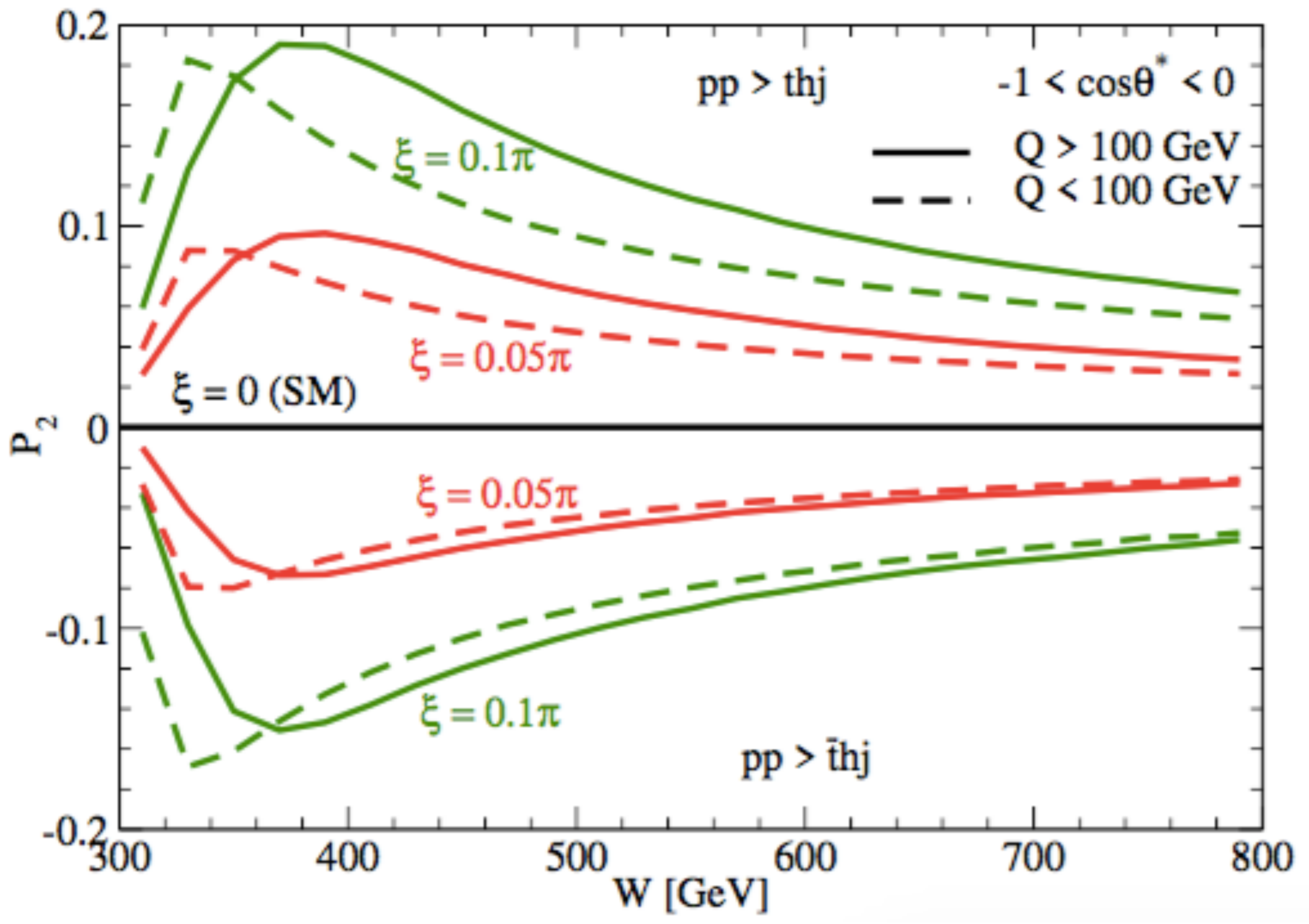

FIG. 15: P_2 v.s. W for $pp \to thj$ (a) and $pp \to \bar{t}hj$ (b) in the region $-1 < \cos\theta^* < 0$. The green curves are for $\xi = 0.1\pi$, while the red curves are for $\xi = 0.05\pi$. The soid curves are for $Q > 100$ GeV, while the dashed curves are for $Q < 100$ GeV.

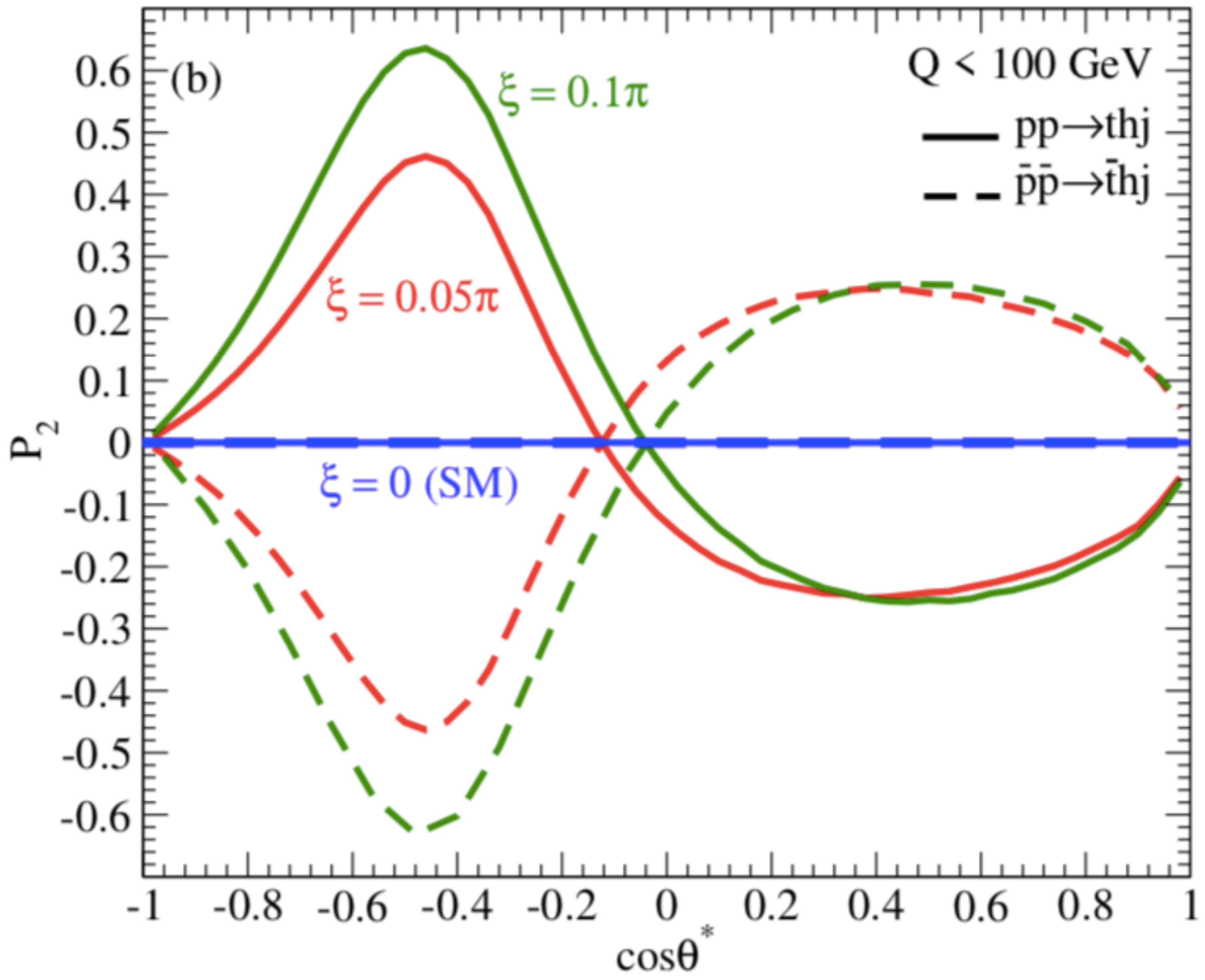

$$pp \to thj \quad (ub \to dth) \quad \overset{\text{CP}}{\longleftrightarrow} \quad \bar{p}\bar{p} \to \bar{t}hj \quad (\bar{u}\bar{b} \to \bar{d}\bar{t}h)$$

In thj and t̄hj production at the LHC, longitudinal contributions ($W^{\pm}(\lambda=0)$) dominate.

$$W^+(\lambda = 0) + b \to t + h \quad \overset{\text{CP}}{\longleftrightarrow} \quad W^-(\lambda = 0) + \bar{b} \to \bar{t} + h$$

Expected number of events @ HL-LHC

	$\sqrt{s}$ 14 TeV	Number of events @$3ab^{-1}$	Decay channel	Branching Ratio	Number of events	
$\sigma(th)+\sigma(\bar{t}h)$	90 fb	270,000	$(b\ell\nu)(b\bar{b})$	0.13	34,000	✓✓
			$(b\ell\nu)(\gamma\gamma,\ell\ell jj,\mu\mu,4\ell)$	0.0011	300	✓✓
$\sigma(t\bar{t}h)$	613 fb	1,840,000	$(bl\nu)(bjj)(b\bar{b})$	0.17	310,000	✓✓✓
			$(bl\nu)^2(b\bar{b})$	0.028	52,000	✓✓✓
			$(bl\nu)(bjj)(\gamma\gamma,\ell\ell jj,\mu\mu,4\ell)$	0.0015	2,800	✓✓✓
			$(bl\nu)^2(\gamma\gamma,\ell\ell jj,\mu\mu,4\ell)$	0.00025	460	✓✓✓

- t>blv mode for CP sensitivity (t vs. $\bar{t}$)
- h decay should not have neutrinos to determine t($\bar{t}$) frame.

	Decay channel	Branching ratio		Decay channel	Branching Ratio	
$t \rightarrow$	bjj	0.67	$h \rightarrow$	$b\bar{b}$	0.58	✓
	$b\ell\nu(\ell = e,\mu)$ ✓	0.22		$\ell\bar{\ell}jj$	0.0025	
	$b\tau\nu$ ✓	0.11		$\gamma\gamma$	0.0023	
				$\mu\bar{\mu}$	0.00022	
				4ℓ	0.00012	

→ 0.0051 ✓

- For a few percent asymmetry measurement, h> bb is necessary

Summary

- Single top+Higgs production is an ideal probe of the top Yukawa coupling because the htt and hWW amplitudes interfere strongly.

- Azimuthal asymmetry between the u>dW+ emission and the W+b>th production planes probes the sign of CP violating phase.

$$A_\phi \sim \int_0^\pi (|M_+|^2 + |M_-|^2) d\phi - \int_{-\pi}^0 (|M_+|^2 + |M_-|^2) d\phi \;\propto\; \sin \xi_{htt}$$

- Polarization can be measured by using the density matrix.

$$\rho_{\lambda\lambda'} = \frac{1}{\int (|M_+|^2 + |M_-|^2) d\Phi} \int \begin{pmatrix} |M_+|^2 & M_+ M_-^* \\ M_- M_+^* & |M_-|^2 \end{pmatrix} d\Phi = \frac{1}{2}\left[\delta_{\lambda\lambda'} + \sum_{k=1}^{3} P_k \sigma^k_{\lambda\lambda'}\right]$$

- Polarization perpendicular to the scattering plane measures the relative phase between the two helicity amplitudes

$$P_2 = \frac{-2\mathrm{Im}(M_+ M_-^*)}{|M_+|^2 + |M_-|^2} \;\propto \sin \xi_{htt}$$

- We find significant asymmetry reaching Aφ ~+8%(th),-10%($\bar{t}$h), whereas P_2~+18% (th), -15% ($\bar{t}$h) for xi=0.1pi. All the asymmetries change sign if ξ is negative.

Backup

A gauge invariant top Yukawa sector

Dimension-6 operator

$$\mathcal{L} = -y_{\rm SM} Q^\dagger \phi t_R + \frac{\lambda}{\Lambda^2} Q^\dagger \phi t_R \left(\phi^\dagger\phi - \frac{v^2}{2}\right) + \text{h.c.}$$

$$Q = (t_L, b_L)^T$$

$$\phi = ((v + H + i\pi^0)/\sqrt{2}, i\pi^-)^T$$

$$\begin{aligned}\mathcal{L}^{\rm SMEFT}_{ttH} =& -m_t t_L^\dagger t_R - g_{\rm SM}\left[(H + i\pi^0)t_L^\dagger + i\sqrt{2}\pi^- b_L^\dagger\right] t_R \\ & -(ge^{i\xi} - g_{\rm SM})\left\{H t_L^\dagger t_R + \frac{H}{v}\left[(H + i\pi^0)t_L^\dagger + i\sqrt{2}\pi^- b_L^\dagger\right] t_R\right\} \\ & -(ge^{i\xi} - g_{\rm SM})\left\{\left[\frac{H^2 + (\pi^0)^2}{2v} + \frac{\pi^+\pi^-}{v}\right] t_L^\dagger t_R \right.\\ & \left. + \frac{H^2 + (\pi^0)^2 + 2\pi^+\pi^-}{2v^2}\left[(H + i\pi^0)t_L^\dagger + i\sqrt{2}\pi^- b_L^\dagger\right] t_R\right\} + h.c.,\end{aligned}$$

$$g_{\rm SM} = \frac{y_{\rm SM}}{\sqrt{2}} = \frac{m_t}{v} \qquad \frac{g_{\rm SM} - ge^{i\xi}}{v^2} = \frac{\lambda}{\Lambda^2}$$

Additional ttHH and ttHHH coupling

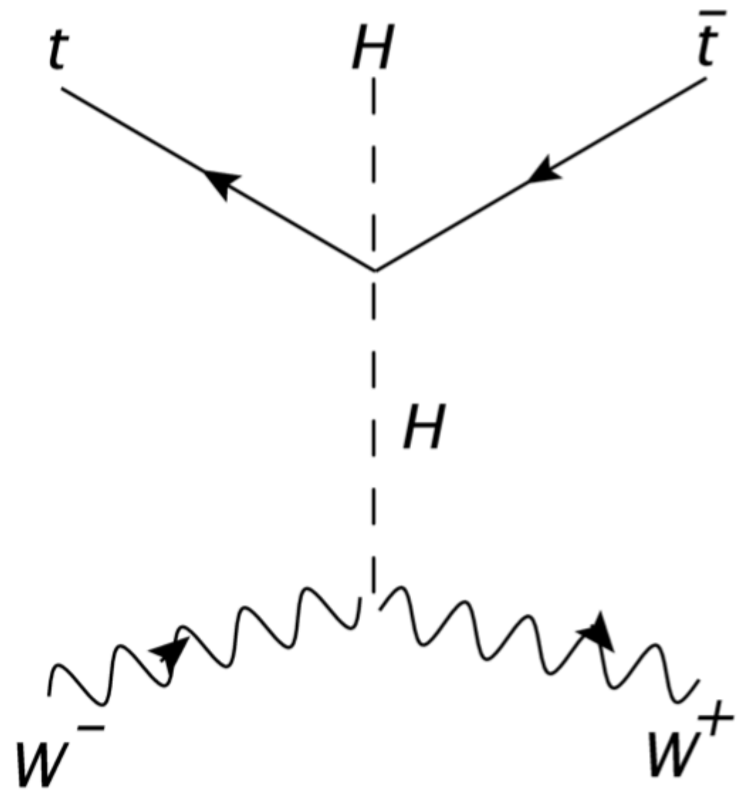

$$\mathcal{L}^{\rm SMEFT}_{ttHH} = \frac{3(g_{\rm SM} - ge^{i\xi})}{v}\frac{H^2}{2} t_L^\dagger t_R + \text{h.c.}$$

Feynman-Diagram (FD) gauge

- Weak bosons are 5-components $W^{\pm M}=(W^{\pm\mu},\pi^{\pm})$, EOM mixes $W^{\pm\mu}$ and $\pi^{\pm}$, unlike in R_ξ gauge.

- FD gauge propagator $$iG_V^{\rm FD}(q)_{MN} = \frac{iP_V^{\rm FD}(q)_{MN}}{q^2 - m_V^2 + i\epsilon}$$

$$P_V^{\rm FD}(q)_{MN} = \begin{pmatrix} -g_{\mu\nu} + \frac{q_\mu n(q)_\nu + n(q)_\mu q_\nu}{n(q)\cdot q} & i m_V \frac{n(q)_\mu}{n(q)\cdot q} \\ -i m_V \frac{n(q)_\nu}{n(q)\cdot q} & 1 \end{pmatrix} \qquad n(q)^\mu_{\rm FD} = ({\rm sgn}(q^0), -\vec{q}/|\vec{q}|)$$

- Helicity ±1 states don't mix with the Goldstone boson. Helicity 0 state is a mixture of

$$-\frac{Q\, n^\mu}{n\cdot q} = \epsilon^\mu(q, h=0) - \frac{q^\mu}{Q}, \quad Q = \sqrt{|q^2|}$$

and the Goldstone boson.

- Because the Goldstone bosons are parts of the physical weak boson, all Goldstone boson vertices contribute to the scattering amplitudes in the FD gauge

[1] Kaoru Hagiwara, Junichi Kanzaki and Kentarou Mawatari, 'QED and QCD helicity amplitudes in Parton-shower gauge.' Eur.Phys.J.C 80(2020) 6, 584
[2] Junmou Chen, Kaoru Hagiwara, Junichi Kanzaki and Kentarou Mawatari, 'Helicity amplitudes without gauge cancellation for electroweak processes'Eur.Phys.J.C 83 (2023).
[3] Junmou Chen, Kaoru Hagiwara, Junichi Kanzaki, Kentarou Mawatari and YJZ, 'Helicity amplitudes in light-cone and Feynman-diagram gauges'Eur.Phys.J.Plus 139 (2024).

ub > dtH amplitudes in the FD gauge

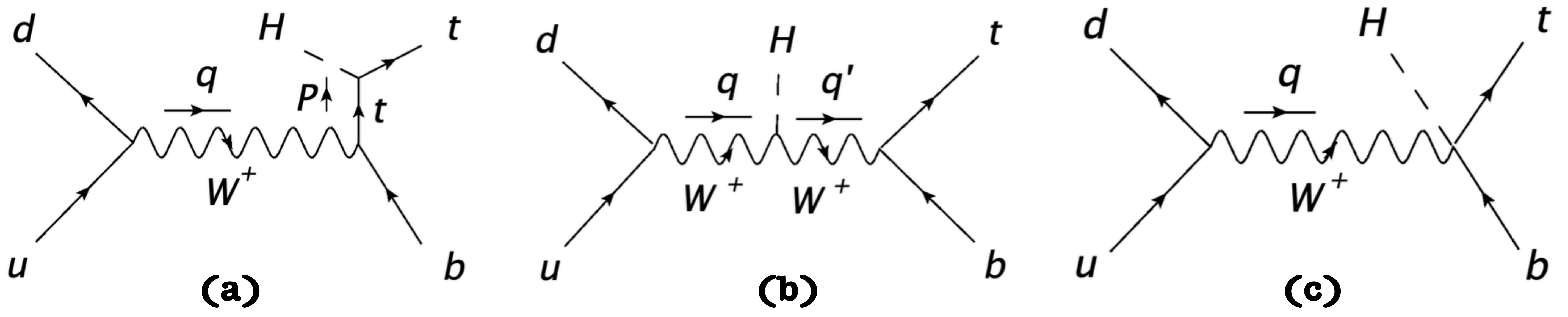

$$\begin{aligned}\mathcal{M}_\sigma &= \mathcal{M}_\sigma^{\mathrm{FD(a)}} + \mathcal{M}_\sigma^{\mathrm{FD(b)}} + \mathcal{M}_\sigma^{\mathrm{FD(c)}} \\ &= \bar{u}(p_d,-)\Gamma^M_{duW}u(p_u,-)G_W^{FD}(q)_{MN}\bar{u}(p_t,\sigma) \\ &\quad \left\{\Gamma_{ttH}G_t(P)\Gamma^N_{tbW} + \Gamma^{NR}_{WWH}(q,q')G_W^{FD}(q')_{RS}\Gamma^S_{tbW} - \Gamma^N_{tbWH}\right\}u(p_b,-)\end{aligned}$$

Preliminary findings:

- **Gauge invariance**

$$\hat{\mathcal{M}}_{h\sigma}^{\mathrm{U(a)}} + \hat{\mathcal{M}}_{h\sigma}^{\mathrm{U(b)}} = \hat{\mathcal{M}}_{h\sigma}^{\mathrm{FD(a)}} + \hat{\mathcal{M}}_{h\sigma}^{\mathrm{FD(b)}} + \hat{\mathcal{M}}_{h\sigma}^{\mathrm{FD(c)}}$$

- **We identify the 'unphysical ' gauge cancellation in the U gauge between $M_U^{(a)}$ and $M_U^{(b)}$.**
- **At high m(tH), the ξ dependence is dominated by $M_{FD}^{(c)}$** $\propto \; y_{\mathrm{SM}} - y e^{i\xi}$